

Nuclear Structure analysis of Heavy-Ion Collisions using Neural Network model

10th Asian Triangle Heavy-Ion Conference - ATHIC 2025
IISER Berhampur, India

Abhisek Saha
Center for High Energy Physics, Peking University

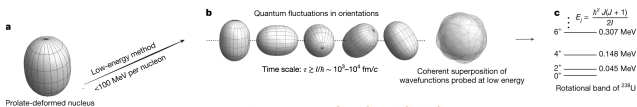
In collaboration with Hadi Mehrabpour, Huichao Song, and Jiangyong Jia



Limitations of Low-Energy Experiments

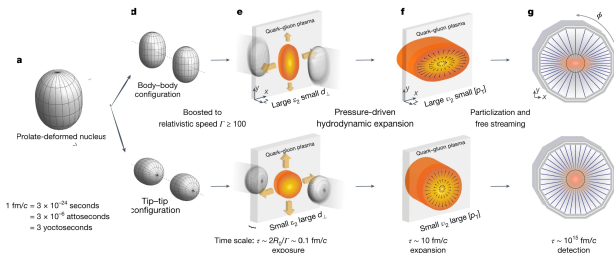
- Experimentally, the deformation of an (even-even) nucleus of mass number A and charge Ze is quantified by,

$$\beta = \frac{4\pi}{3ZeR_0^2} \sqrt{B(E2)} \uparrow, \quad R_0 = 1.2A^{1/3},$$
 $B(E2) \uparrow \rightarrow$ measured transition probability of the electric quadrupole operator from the ground state to the first 2^+ state.



STAR, Nature 635, 67–72 (2024)

- In ground states, nuclear shapes may fluctuate. Over different timescales with a period of $\tau_{rot} \approx 10^3 - 10^4 \text{ fm/c}$ ($1 \text{ fm/c} = 3 \times 10^{-24}$ seconds), much shorter than Spectroscopic processes.
- Spectroscopic measurements integrate over all nuclear orientations.
- Charge distribution only reflects an averaged deformation. Cannot provide real-time insights into dynamic nuclear shape fluctuations.
- Heavy-ion collision experiments operate on much shorter ($\sim 10^{-24}$ s) timescales and provide many body nucleon interactions in each nucleus.



STAR, Nature 635, 67–72 (2024)

Nuclear Structure



Spatial anisotropy at the initial state



Momentum anisotropy of the distribution of emitted particles

Initial state parameters:

Initial Size: $R_\perp \propto \langle r_\perp^2 \rangle$ Initial Shape: $\mathcal{E}_n \propto \langle r_\perp^n e^{-in\phi} \rangle$

Final State momentum anisotropy:

$$\frac{d^2 N}{d p_T d \phi} = \frac{d N}{2 \pi d p_T} \left(1 + 2 \sum_{n=1}^{\infty} V_n(p) e^{in\phi} \right)$$

Prolate

$$\beta_2 = 0.25, \cos(3\gamma) = 1$$



Triaxial

$$\beta_2 = 0.25, \cos(3\gamma) = 0$$



Oblate

$$\beta_2 = 0.25, \cos(3\gamma) = -1$$



Approx linear response EBE

$$\text{at H.E. } \frac{\delta[p_T]}{[p_T]} \propto -\frac{\delta R}{R}$$

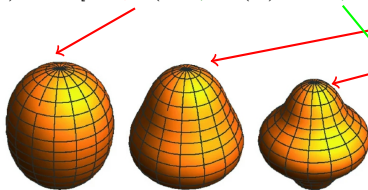
$$V_n \propto \mathcal{E}_n$$

Jiangyong Jia, Phys.Rev.C 105 (2022) 4, 044905

Woods-Saxon profile to include intrinsic deformations:

$$\rho(r, \Theta, \Phi) \propto \frac{1}{1 + \exp\left(\frac{r - R(\Theta, \Phi)}{a}\right)},$$

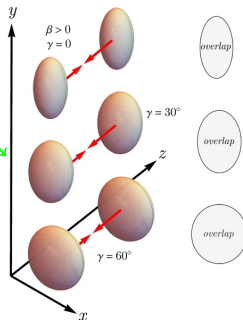
$$R(\Theta, \Phi) = R_0 [1 + \beta_2 (\cos \gamma Y_{20}(\Theta) + \sin \gamma Y_{22}(\Theta, \Phi)) + \beta_3 Y_{30}(\Theta) + \beta_4 Y_{40}(\Theta)]$$



Triaxial Spheroid: $a \neq b \neq c$

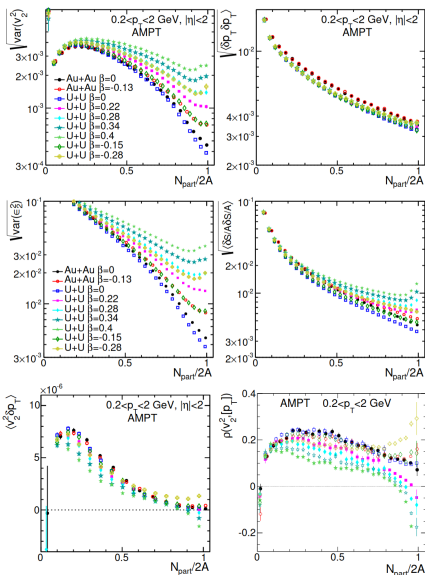
Prolate : $a = b < c \rightarrow \beta_2, \gamma = 0$

Oblate : $a < b = c \rightarrow \beta_2, \gamma = \pi/3$ or $-\beta_2, \gamma$



B. Bally et al. Phys. Rev. Lett. 128,082301 (2022)

Observable dependencies on deformation



→ The variance of $\langle v_2^2 \rangle$ strongly depends on β_2 deformation, reflecting a predominantly linear response to the eccentricity fluctuations.

Giacalone et al., *Phys. Rev. Lett.* 127, 242301 (2021)

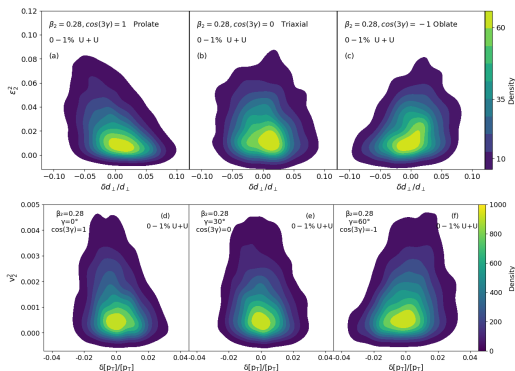
→ The variance of $\langle [p_T] \rangle$ exhibits only a very modest dependence on quadrupole deformation → 0 – 10% increase for $\beta_2 = 0 - 0.4$ J. Jia, *Phys.Rev.C* 105, 014905 (2022)

→ Non-trivial dependence: For prolate deformation $\beta_2 > 0$, the covariance decreases with increasing β_2 values. However, for oblate deformation $\beta_2 < 0$, the covariance increases for more negative β_2 value in central collisions but decrease in mid-central and peripheral collisions..

J. Jia et al., *Phys. Rev. C* 105, 014906 (2022)

→ Both v_2^2 and ϵ_2^2 are similar between $\beta_2 = -0.28$ and $\beta_2 = 0.28$, implying they are mostly even functions of β_2

Comparison bw the initial- and final-state distributions



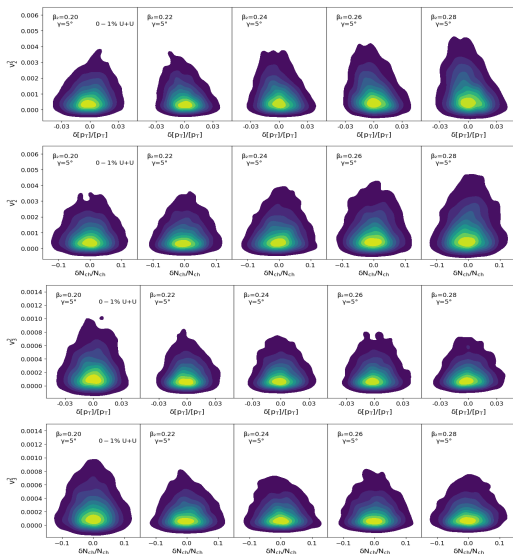
Top Row: $\epsilon_2 - \delta d_{\perp}/d_{\perp}$ with different γ at fixed $\beta_2 = 0.28$

Bottom Row: $v_2^2 - \delta[p_T]/[p_T]$ correlations

$\langle \epsilon_2^2 \delta d_{\perp} \rangle < 0$ for prolate nuclei
 $\langle \epsilon_2^2 \delta d_{\perp} \rangle \sim 0$ for rigid triaxial nuclei
 $\langle \epsilon_2^2 \delta d_{\perp} \rangle > 0$ for oblate nuclei

- The final-state observables demonstrate a similar dependence on the initial-state deformation, reflecting how initial anisotropies influence the resulting flow patterns in the final state.
- The comparison highlights how both initial- and final-state observables encode nuclear structure information, offering unique perspectives on the role of deformation in heavy-ion collision outcomes.

Role of β_2 deformation in influencing the flow correlation observables



→ As β_2 increases, the distributions become broader and expands significantly along the v_2^2 .

→ No broadening along the $\delta[p_T]/[p_T]$ and $\delta N_{ch}/N_{ch}$ axis.

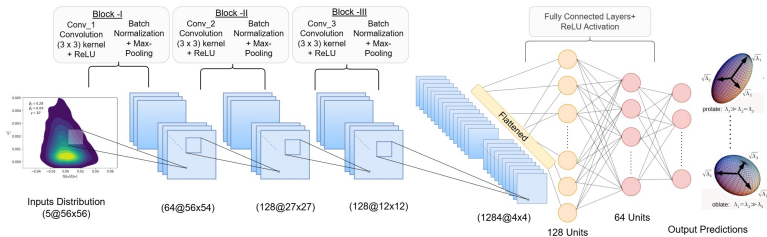
→ In the presence of deformation, multiplicity distributions $p(N_{part})$ are expected to be broadened and smeared out but the total volume of the nucleus slightly increases.

→ The central region of the distribution, corresponding to higher event density, shifts and stretches with increasing deformation parameters, but the overall size in the x-axis remains largely unchanged.

→ v_3^2 does change but no pattern was observed.

Neural Network Architecture

- **Architecture:** A simple yet efficient neural network with multiple layers, including convolutional layers for feature extraction and fully connected layers for classification.



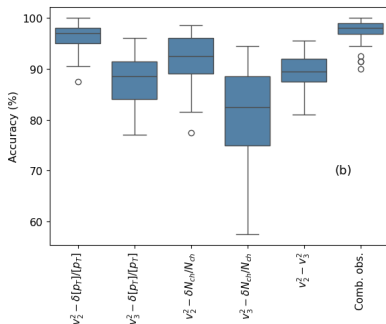
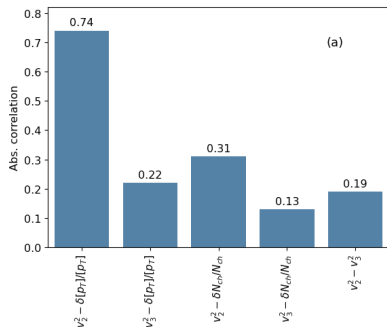
- Use nuclear deformation-dependent correlations to train the neural network.
- Initial-state: $\epsilon_2^2 - \delta d_{\perp} / d_{\perp}$.
 - Final-state: $v_2^2 - \delta[p_T] / [p_T]$, $v_3^2 - \delta[p_T] / [p_T]$, $v_2^2 - \delta N_{ch} / N_{ch}$, $v_2^2 - v_3^2$, etc.
- Converting observables into images for neural network training.
(Captures correlations between observables and maps them into a format suitable for convolutional layers.)

Key Objectives for Data Preparation

- Provide the model with diverse nuclear shapes and configurations.
 - ⊗ Created 40 groups, each defined by a unique combination of deformation parameters β_2 , β_4 , and γ .
 - ⊗ β_2 : Varied from 0.2 to 0.3 in 0.02 increments and included negative values from -0.22 to -0.28 .
 - ⊗ γ : Assigned discrete values of 5° , 10° , 15° , and 20° .
 - ⊗ $^{238}\text{U} + ^{238}\text{U}(\sqrt{s_{NN}} = 193)\text{GeV}$, $^{129}\text{Xe} + ^{129}\text{Xe}(\sqrt{s_{NN}} = 5.44)\text{TeV}$.
- For each β , γ combinations, we simulated 10^6 U+U collision events using iEBE-VISHNU under minimum-bias conditions with a 0 – 1% centrality cut to select ultra-central collisions.
- Randomly selected 20 – 30% of events from each configuration to generate 3,000 images per configuration.

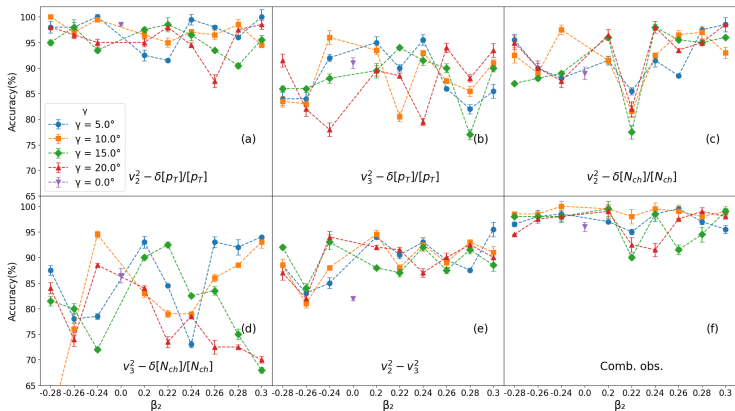
Correlations vs Accuracy

We can quantify the correlation using the pearson correlation Sensitivity of each observable to the deformation and its suitability for training.

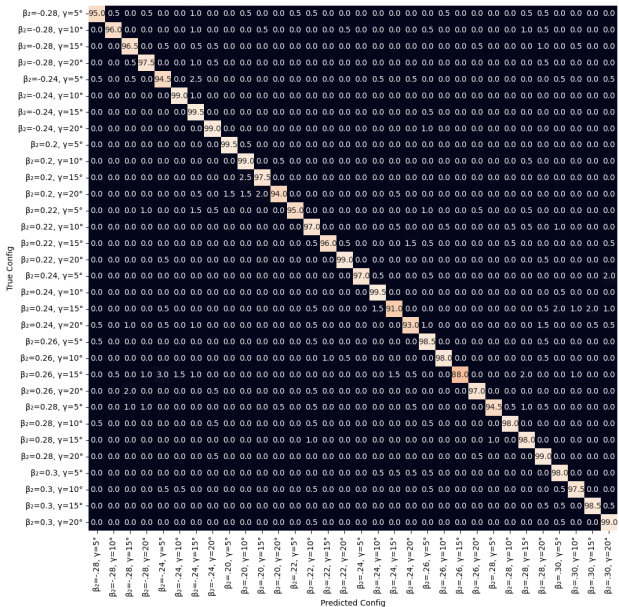


- ➔ Observables related to v_3^2 correlations are less sensitive with the change in nuclear deformations as v_3 receives limited contributions from quadrupole deformation
- ➔ Observables with higher mean correlations lead to higher prediction accuracy.
- ➔ The combined observables category where all the correlations are used as input to the network, achieve consistently high accuracy, with a narrow box and shorter tails.

Prediction of β and γ based on various final-state correlations



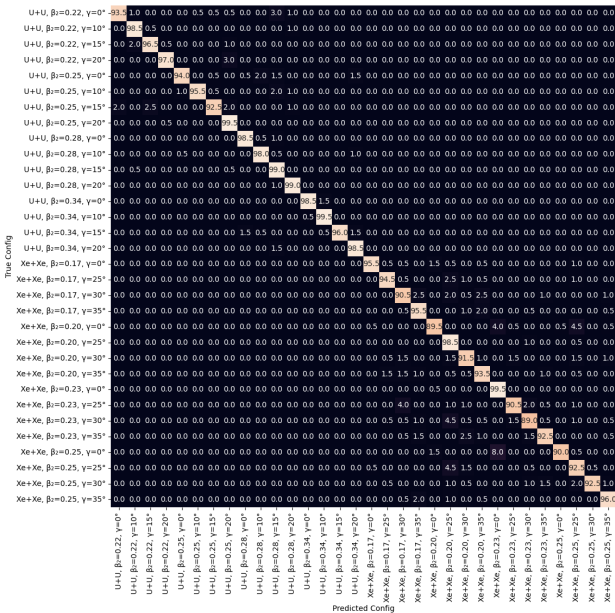
- The accuracy range varies significantly depending on the type of observable distributions used for training NN.
- $v_2^2 - \delta[p_T]/[p_T]$ correlation demonstrates high and consistent classification accuracy.
- Correlations involving v_3^2 result in poor training.
- The upper bound breaks for combined observables.

Confusion Matrix for $^{238}\text{U} + ^{238}\text{U}$ 

→ For almost all values of β_2 and γ , the prediction accuracies exceed 95%. This indicates that the performance of the neural network does not significantly depend on the specific deformation parameters.

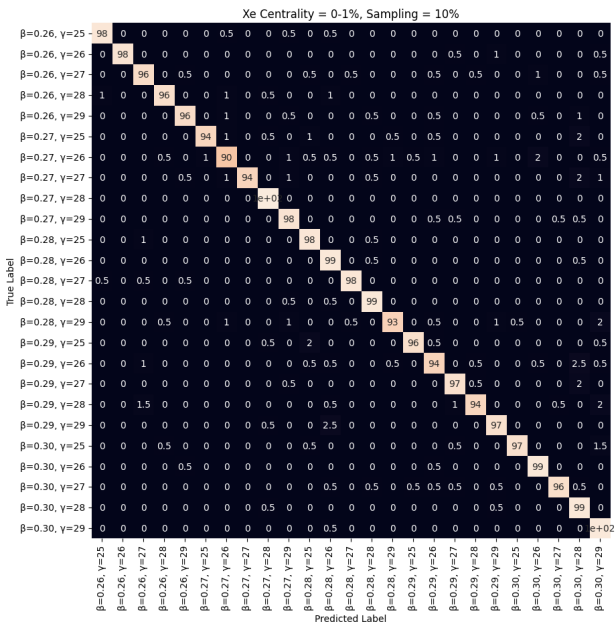
→ The misclassifications are relatively rare, as indicated by the dominance of high diagonal values and the near-zero values off the diagonal.

Confusion Matrix for $^{238}\text{U} + ^{238}\text{U}$ and $^{129}\text{Xe} + ^{129}\text{Xe}$



- We combined two distinct nuclear collision systems to assess the network's robustness against variations in nuclear size.
- Obtained from the initial-state correlation in Xe+Xe and U+U collisions.
- Lowest Prediction accuracy: 89%
- The model is robust across different system sizes.

Confusion Matrix for $^{129}\text{Xe} + ^{129}\text{Xe}$ with smaller $\delta\beta_2$ and $\delta\gamma$



→ Performed tests using a smaller range of β and γ with finer steps ($\delta\gamma = 1^\circ$, $\delta\beta = 0.01$) while employing initial-state observables, and observed consistently high prediction accuracy.

→ Lowest Prediction accuracy: 90%

Summary

- Our work establishes a systematic framework for using heavy-ion collision observables in nuclear structure studies, providing valuable insights into the connection between final-state dynamics and nuclear deformations.
- We demonstrated the sensitivity of observables, such as v_2 , $[p_T]$, and their correlations, to nuclear structure.
- For the first time, a neural network has been successfully applied to extract nuclear structure information, specifically deformation parameters, from heavy-ion collision data.
- Validated on multiple collision systems (U+U and Xe+Xe) and observables, demonstrating generalization across nuclear sizes and configurations.

Acknowledgment:

This work is supported by the National Natural Science Foundation of China with grants Nos.12247107, 12075007

Thanks!